Case Studies in Thermal Engineering 26 (2021) 101115

Contents lists available at ScienceDirect

Case Studies in Thermal Engineering

journal homepage: www.elsevier.com/locate/csite

Thermodynamic optimization of a rack-level water-cooling infrastructure in high load data centers based on the principle of minimum exergy destruction

Hao Tian [a], Hong Zheng [b], Jialiang Yang [a,*]

[a] Institute of Optics, Fine Mechanics and Physics, Chinese Academy of Sciences, Changchun, Jilin, 130033, China
[b] School of Aerospace Engineering, Tsinghua University, Beijing, 100083, China

ARTICLE INFO

Keywords:
Server
Data center
Heat transfer
Exergy
Optimization
Case study

ABSTRACT

Exergy model and the least exergy loss principle are introduced to analyze the exergy loss distribution in heat transfer and air/water flow process, for a combined server/cabinet cooling network. Based on the optimized case suggested by the exergy model, a multi-stage water cooling scheme is designed, with two-stage heat exchanger in server cabinet, and double-chiller in the water loop. Both thermal and energy performance of such cooling infrastructure has been tested in a data center in China, with the measured performance in good agreement with the designed values, and the exergy loss model has been validated.

1. Introduction

The past decade has witnessed the fast growth of data center power consumption, accounting for approximately 1.3%–1.5% of global energy use [1]. About one third power is spent on cooling system, which means an annual amount of 130 TWh electric power is consumed just to remove the heat dissipated inside data centers. For the high load data centers (averagely 10–15 kW for each rack), a small improvement in cooling performance brings a significant reduction in total energy consumption.

Inefficiencies in air flow management greatly affects cooling performance and energy cost, such as hot air recirculation and cold air bypass [2]. To evaluate such inefficiencies, most literature uses energy assessment and temperature-based metrics, such as supply heat index *SHI*, return heat index *RHI*, rack cooling index *RCI* and so on [3–5]. The first law-based analysis reveals the temperature field and cooling energy distribution, e.g., how much energy is consumed by chillers, fans and hot air recirculation/cold air bypass.

However, such method does not quantify the irreversibility itself [6,7].Neither the temperature field nor the energy cost can describe the waste of available cooling potentials in each heat transfer process, from chip-level to space-level [8]. This is precisely the focus of energy-saving analysis. This disadvantage makes the firs law-based method insufficient to design optimal cooling infrastructures with higher energy performance [9]. To better characterize the energy inefficiencies caused by thermal irreversibility, the second law of thermodynamics provides a more suitable approach. Compared with energy cost and temperature field, the concept of exergy destruction is more suitable to precisely quantify the loss of available cooling potentials and draws an exergy destruction map of data centers. Such exergy destruction map identifies where the largest irreversibility occurs, where truly deserves improvement. Compared with the first-law method, the exergy destruction analysis does not focus on energy cost assignment, it focuses on how much

* Corresponding author.
E-mail addresses: tianh@ciomp.ac.cn (H. Tian), hong-zhe20@tsinghua.edu.cn (H. Zheng), yangjialiang20@mails.ucas.ac.cn (J. Yang).

https://doi.org/10.1016/j.csite.2021.101115
Received 24 March 2021; Received in revised form 13 May 2021; Accepted 26 May 2021
Available online 1 June 2021

Nomenclature

$Q =$	server dissipated heat
$Q_{HEX} =$	exchanged heat
$HEX =$	heat exchanger
$T_a =$	air inlet temperature
$T_{w,in} =$	inlet water temperature
$T_{w,out} =$	outlet water temperature
$T =$	motherboard surface temperature
$\overline{T}_a =$	average temperature of the air along the surface of the motherboard
$T_o =$	air outlet temperature
$T_0 =$	reference temperature of zero-exergy state
$\Delta T_{\mathrm{m}} =$	logarithmic mean temperature difference between cooling water and air
$m =$	air outlet temperature air mass flow rate
$m_{HEX} =$	air mass flow rate through the heat exchanger
$c_p =$	air specific heat
$\rho =$	air density
$L =$	length of server motherboard
$D =$	equivalent hydraulic diameter of server inlet
$A =$	heat dissipation area of server motherboard
$f =$	mean frictional coefficient
$S_t =$	Stanton Number
$h =$	convective heat transfer coefficient
$V =$	mean air velocity
$P_{\mathrm{in}} =$	inlet air pressure of the heat exchanger
$P_{\mathrm{out}} =$	outlet air pressure of the heat exchanger
$R =$	universal gas constant, 8.314J/(mol.K)

available cooling potential can be saved. The more cooling potential saved. the more available chiller work can be reduced. From this perspective, the exergy model precisely ensures the maximum return on investment, and guides the optimal energy-saving design in a more effective way.

Exergy destruction has been used to analyze and optimize various heat transfer processes. To improve data center cooling inefficiency, Shah et al. [10–14] analyzed the exergy destruction distribution at different heat transfer components. Shah used the least exergy destruction principle to get the optimal heat transfer parameters at component-level in data centers. These parameters have been compared with other research to testify the least exergy destruction principle.

The work by Refs. [15–20] built models of exergy destruction in typical data center cooling infrastructures, using energy and exergy balance. The above work analyzed the exergy destruction of data center cooling at system-levels, and compared the exergy destruction variation with different boundaries, including rack number, rack load, air-flow pattern, cooling strategies and chiller working mode. As for the air-mixing exergy destruction, work by Refs. [21–23] integrated exergy balance equation into CFD governing equations and computed the exergy destruction distribution among data center space, under different cooling architectures, air paths and data center layouts. The above work revealed the characteristics of exergy destruction in different heat transfer process and different levels in data center cooling, and combined the component-level models and component operating parameters into exergy models.

Although legacy architectures employ room-based cooling architectures, the RMCU is promising for high-density computing infrastructure [24–26]. Such a scheme consists of a rack-mountable cooling system placed inside each rack that has separated hot and cold chambers. A version of the RMCU suitable for a high density scalable modular DC is the IRC that simultaneously delivers cooling air to several racks to reduce hot-spots [27,28]. The IRC architecture is an enclosed row-based cooling solution that provides cold air to several IT racks stacked beside one another. Placing the cooling units nearer to the heat sources, i.e., the servers, reduces the airflow path length, which in turn reduces the adverse effects due to pressure drops. Doing so also reduces hot and cold air mixing. An exergy-based assessment of the improvement in energy consumption by a modular (i.e., RMCU and IRC) DC as compared to a legacy DC is yet unavailable. Hence, there is a lack of guidance for DC designers for selecting a suitable cooling architecture. This leads to cooling overdesign, often by a factor greater than two, producing energy waste and considerably increasing the total cost of ownership (TCO).

The work above analyzed exergy distribution and variation law in data center heat transfer path, from chip to room. However, most exergy analysis is based on the single component models off the shelf, e.g., server exergy model, rack exergy model, heat exchanger exergy model, airflow exergy model and so on. So far, very few work is reported to perform a further optimization with a combination of new created component-level exergy models, using the least exergy destruction principle. Such creative work not only characterizes the inner law of exergy behavior for system level, it also suggests the optimal operation strategies and operating parameters in forms of minimum exergy destruction.

A methodology that compares different cooling architectures based on their contributions to exergy destruction is proposed.

Combining the existed exergy models of servers, heat exchangers and airflows together, a new rack-level exergy model is built to optimize both the heat transfer path and rack-level cooling infrastructures.

2. Exergy modeling of rack-level cooling

Shah [40] studied the exergy destruction characteristics of air-cooling process inside the rack, and proposed the server-level exergy model as follows [29].

$$\dot{\psi}_{total}=\dot{\psi}_{heat}+\dot{\psi}_{flow}=\frac{\dot{Q}^2}{L\dot{M}c_p}\frac{D}{S_t}\frac{T_a}{\overline{T}_a^2}+\frac{8\dot{m}^3 L}{\rho^2}\frac{f}{DA^2}\frac{T_a}{\overline{T}_a} \quad (1)$$

$$\overline{T}_a=T_a+\frac{(T-T_a)-(T-T_o)}{In\left(\frac{T-T_a}{T-T_o}\right)} \quad (2)$$

$$S_t=\frac{h}{\rho V c_p} \quad (3)$$

Terms of Q, h and$T-\overline{T}_a$are governed by Newton's law of cooling as follows [29].

$$\dot{Q}=hA\left(T-\overline{T}_a\right) \quad (4)$$

Combine equation (2)~(4) into equation (1), with $\dot{m}=\frac{\pi}{4}\rho VD^2$ [29].

$$\dot{\psi}_{total}=\dot{\psi}_{heat}+\dot{\psi}_{flow}=\frac{4A}{\pi DL}\frac{D}{S_t}\frac{\left(T-\overline{T}_a\right)}{\overline{T}_a^2}\dot{Q}+\frac{8\dot{m}^3 L}{\rho^2}\frac{f}{DA^2}\frac{T_a}{\overline{T}_a} \quad (5)$$

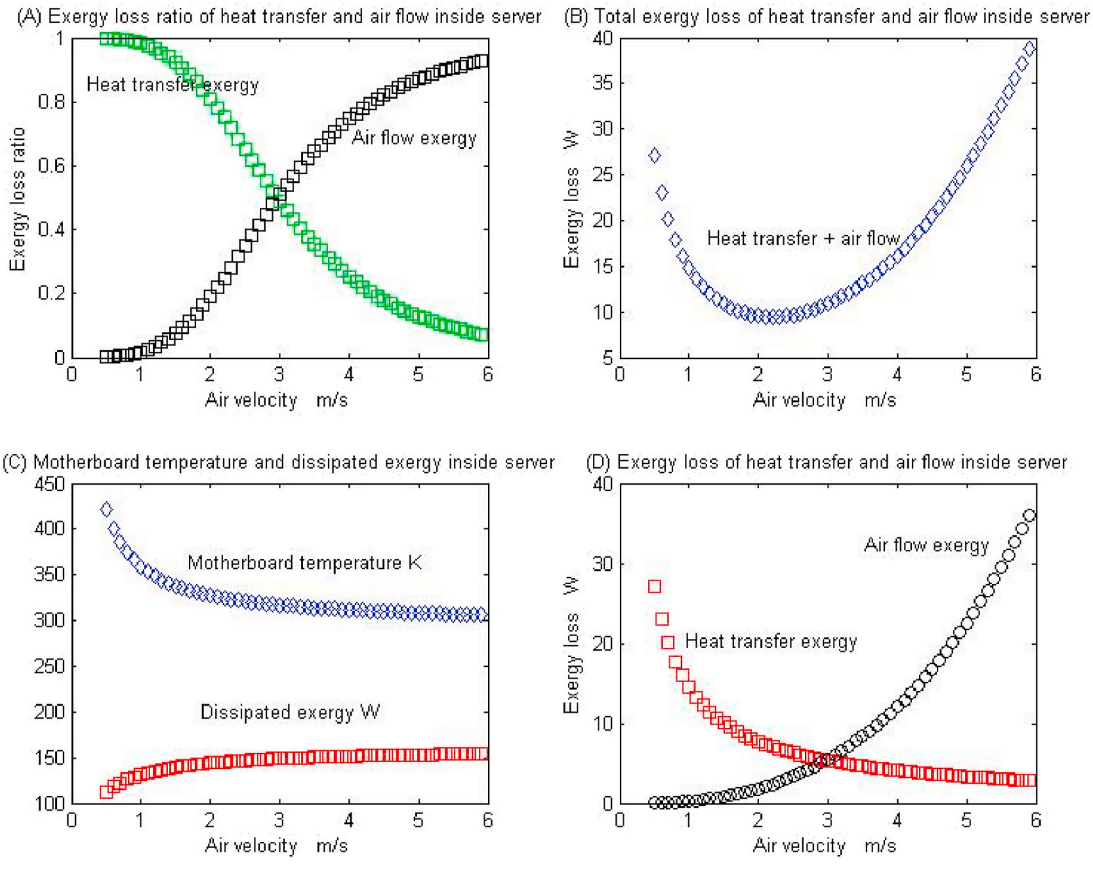

Fig. 1. Exergy destruction law of rack-level air-cooling process.

Given the parameters of Q, L, D, A and T_a, the exergy destruction law of rack-level air cooling is illustrated by Fig. 1.

Fig. 1 shows that, as the flowrate of cooling air increases, the temperature difference between server and air keeps decreasing, the exergy destruction caused by heat transfer resistance decreases. Meanwhile, the exergy destruction caused by airflow resistance increases. The total exergy destruction drops then raises. Such parabolic trend indicates the potential for further optimization of air flowrate.

Fig. 1 tells the minimum total exergy destruction occurs at air velocity of 2.4 m/s. At this optimum velocity, the motherboard temperature dropped from initial 400 K–324 K, quite close to the lowest temperature (307 K). Meanwhile, the exergy dissipation by the irreversible change from high-grade electric power into low-grade heat energy also reaches145.4 W, very close to the highest value (154.1 W). Such maximum exergy dissipation indicates that most of the input electric power has been turned into useful fan work, with very small part irreversely consumed by resistance of air flow and heat transfer. In other words, the optimal thermodynamic efficiency of rack-level cooling scheme occurs at air velocity of 2.4 m/s.

When cooling water temperature remains higher than air dew point temperature inside the rack, above rack-level cooling model can be simplified as Fig. 2.

According to exergy balance equation$\dot{\Psi}_d = \dot{\Psi}_{in} - \dot{\Psi}_{out}$, assuming air to be ideal gas, total exergy destruction inside the heat exchanger can be calculated as follows [5].

$$\dot{\psi}_d = \dot{\psi}_{heat} + \dot{\psi}_{flow} = \left(\frac{T_o}{T_o + \Delta T_m}\right)\dot{Q}_{HEX} - \dot{m}_{HEX}\, T_o\left(c_p In\left(\frac{T_m}{T_{out}}\right) - RIn\left(\frac{P_{in}}{P_{out}}\right)\right) \tag{6}$$

$$\Delta T_m = \frac{\left(T_{in} - T_{w,o}\right) - \left(T_{out} - T_{w,in}\right)}{In\left(\frac{T_{in} - T_{w,o}}{T_{out} - T_{w,in}}\right)} \tag{7}$$

Given the server heat, area of heat exchanger and cooling water flowrate, impact of air velocity and water inlet temperature on the exergy destruction inside the heat exchanger is illustrated by Fig. 3.

Fig. 3 shows that, the proportion of exergy consumed by flow resistance increases with the increasing air velocity and decreasing water inlet temperature. Under the same condition, the exergy consumed by flow resistance is always smaller than that consumed by heat transfer resistance. Therefore, the total exergy destruction inside the heat exchanger decreases with the increasing air velocity and decreasing water inlet temperature. This conclusion guides the optimal design of rack-level heat transfer, along with the minimum exergy destruction principle.

3. Optimal design of rack-level cooling infrastructure

The inlet cooling water is set as the reference state of zero-exergy, with the temperature given as 283K. Given the area and heat in the heat exchanger, the optimal water and air velocity can be found by the minimum exergy destruction law.

Besides the optimal fluid parameters, to further reduce the exergy destruction, a new rack-level cooling infrastructure with multi-heat-exchanger configuration is proposed. The number and area of heat exchangers become two key parameters to be optimized. Given the total area and inlet water temperature of 283K, 4 typical cooling cases are designed, composed of 1 single-heat-exchanger configuration and 3 double-heat-exchanger configurations. The detailed information is listed by Table 1.

The heat transfer Q_{HEX}=160W, the total heat exchanger area NTU=2.0 (NTU= NTU_1+ NTU_2). The inlet water temperature (283K) is set as the zero-exergy state temperature. The water flowrate and corresponding air velocity is governed by $\triangle T_w = \triangle T_{air}$, which enables the best thermal match of two fluids.

Fig. 4 demonstrates the optimal air velocity for each cooling case, suggested by the minimum exergy destruction law.

The minimum exergy destruction of cooling case 1 to case 4 is 26.39W, 25.74W, 25.87W and 25.81W. The corresponding optimal air velocity is 2.42 m/s, 2.35 m/s, 2.38 m/s and 2.36 m/s.

Fig. 4 shows that, with the same fluid parameters, compared with case 1, case 2 to case 4 further reduce exergy destruction by

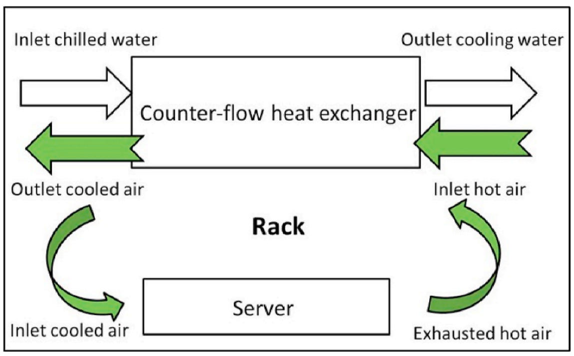

Fig. 2. Simplified rack-level cooling model.

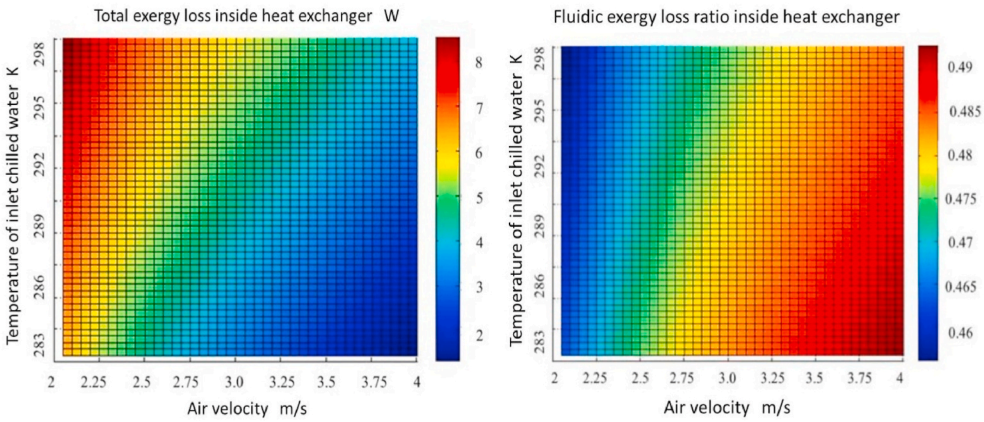

Fig. 3. Exergy destruction distribution inside heat exchanger.

Table 1
Design of four typical cooling configurations.

Cooling case	Number of heat exchangers N	NTU_i (i=1,2 … N)	Inlet water temperature K	Water mass flow rate kg/h	Air velocity m/s
Case 1	N=1	100%	283	1.28–16.70	0.5–6.5
Case 2	N=2	NTU_1:NTU_2=20%:80%			
Case 3	N=2	NTU_1:NTU_2=50%:50%			
Case 4	N=2	NTU_1:NTU_2=70%:30%			

0.5W–0.6W. In other words, the double-heat-exchanger configuration shows higher exergy efficiency and better energy performance than the single-heat-exchanger configuration.

It also can be seen from Fig. 4, compared with the highest exergy destruction (about 110W), the optimal case (about 26W) reduces about 84W and 76% of maximum available useful work, which can be theoretically extracted to offer more cooling capacity.

Fig. 5 shows fan power and exergy destruction curve at above air velocity range. It tells that, the minimum exergy destruction state (about 26W) corresponds to fan power of 5.3W and server temperature of 332K. In contrast, the maximum exergy destruction (about 110W) occurs at air velocity about 6.5 m/s, with fan power of 52W and server temperature of 302K. This means a maximum energy saving potential of 131W (84W + 47W) is available.

For above 3cooling cases of double-heat-exchanger configurations, exergy destruction can be further reduced by optimizing the allocation of heat exchanger area, which is represented by *NTU*. With the optimal *NTU* ratio of two heat exchangers by 0.2/0.8, case 2 further reduces about 0.1W exergy destruction than case 3 and case 4. By contrast, the optimal cooling infrastructure of case 2 saves 0.6–0.7W more available work or potentially useful energy than case 1, with total heat transfer of 160W.

According to the exergy model above, for a 10 kW loaded rack, the maximum exergy destruction saving potential can be 37.5W. Referred to zero-exergy state, such 37.5W of exergy destruction saving can be extracted to drive a reversed Carnot cycle to offer about 152W extra cooling capacity (assuming *COP*=4), which helps to reduce the *PUE* value by about 3.5%.

4. Case study

Based on the optimal rack-level cooling infrastructure above, a two-stage water-cooled rack is designed, assembled and tested in a 570 m^2 data center in Changchun, northeast of China. Fig. 6 shows the photos of the tested racks.

The heat exchanger is a cobber cooling coil filled with chilled water, the fisrt coil is installed behind the front door of the rack to cool intake air, while the second coil installed at the rear door to cool down the rack exhausted air. To better regulate the air flowrate through each server layer inside the rack, 16 units of fans are installed behind the rear coil. Speed of each fan unit can be independently adjusted according to server workload change monitored.

The front coil (referred as first-stage heat exchanger in Fig. 6)pre-cools the rack intake air of room level (~25 °C) to the server preferred cooling air level (~20 °C), using the chilled water (~15 °C) supplied by chiller 1. The rear coil (referred as second-stage heat exchanger in Fig. 6) cools the server exhausted hot air (~45 °C) back to room level (~25 °C) again and discharge into room space, using the outlet water of the front coil with higher cooling temperature (~20 °C). The hot outlet water of rear coil (~28 °C) flows back to chiller 2 and finishes this two-stage cooling loop.

The testing configuration is demonstrated by Fig. 7. Three lines of 60 racks (20 racks for each line) are connected in parallel, forming a double-chiller cooling water loop. Water loop parameters, such as cooling load, flowrate, pressure and temperature, can be regulated through the valves and the two chillers, in accordance with the change of rack workload.

Compared with single chiller, the double-chiller configuration earns more energy benefits from chiller co-operation with variable

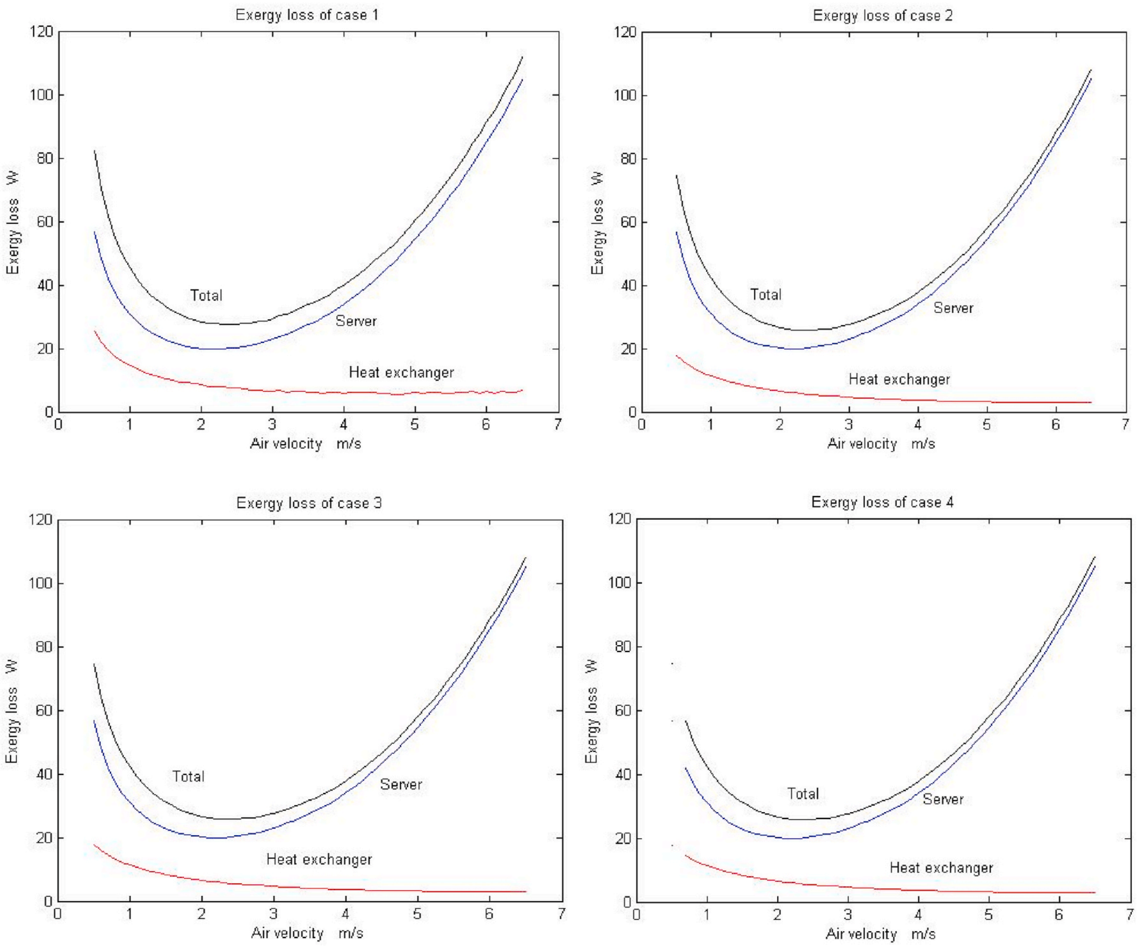

Fig. 4. Optimized exergy state for each cooling case.

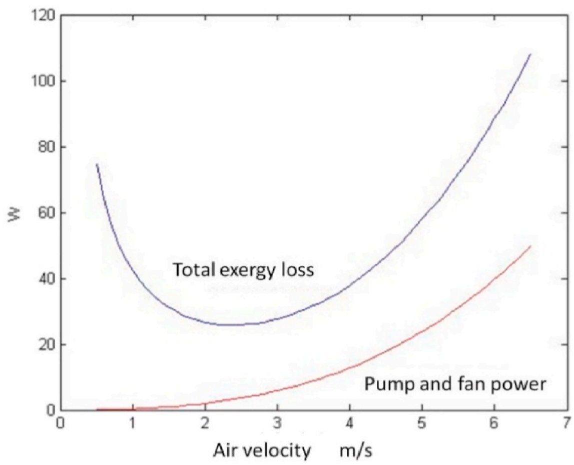

Fig. 5. The fan power curve with air velocity.

cooling load, which ensures at least one chiller offers higher temperature chilled water with higher *EER*. To further improve the energy performance, the water loop uses operating mode of small flow and large temperature difference.

The averaged rack workload is measured as 35 kW. Fan power and pump power are approximately proportional to water flowrate. The rated cooling capacity of each chiller is 50 kW. Table 2 and Table 3 show the optimal parameters of the water loop, suggested by

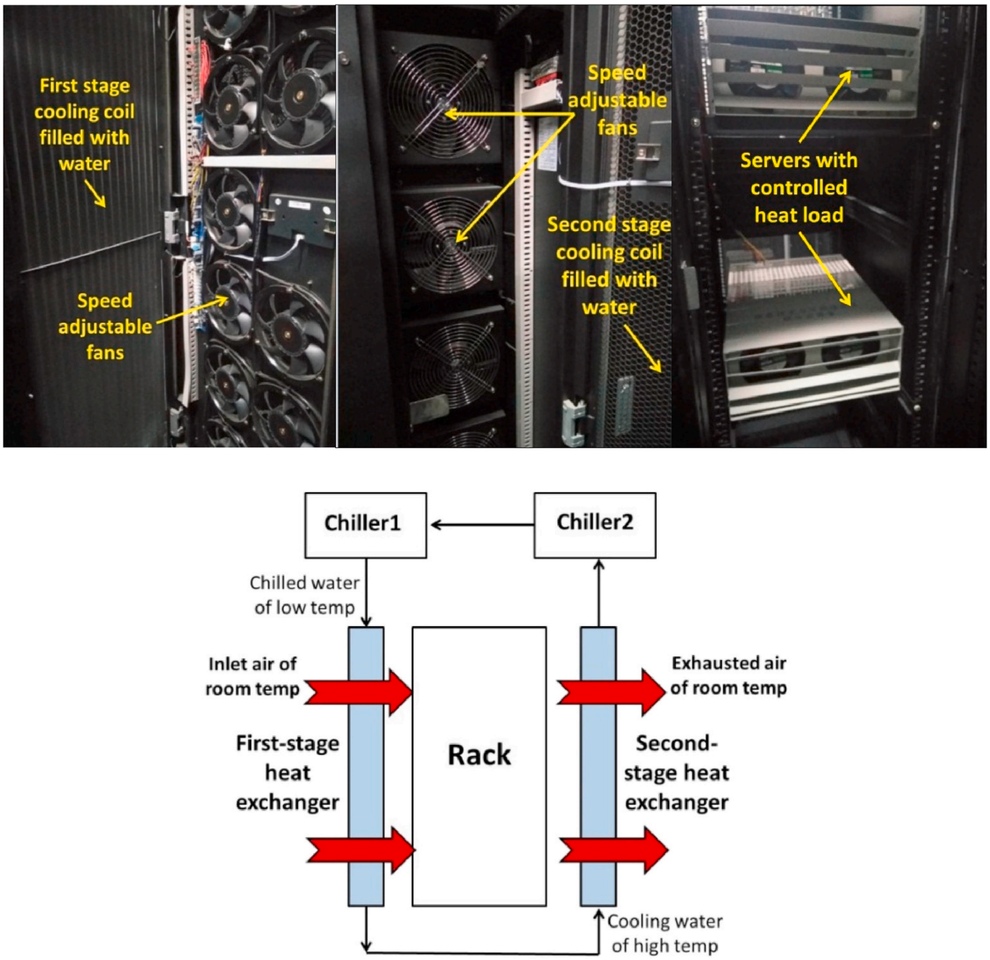

Fig. 6. Photo and schematic diagram of the two-stage water-cooled rack.

the minimum exergy destruction law. The outdoor daily temperature data are measured at July 2018 and January 2019.

To verify the exergy suggested parameters above, performance testing was performed in a 570 m^2 data center in Changchun, Jilin Province, northeast of China, from 2018 to 2019. Among these tests, parameters of the best performance are selected and listed by Table 4 and Table 5. These measured parameters will be used to validate the exergy analysis model.

It can be seen from Tables 4 and 5 that, the measured thermal and energy performance of the combined water loop and the double-stage water-cooling infrastructure show a good agreement with the values predicted by exergy model.

5. Error analysis

The measurement of each workload percentage lasts for at least 48 h. Chiller cooling load and bypass payload are indirectly measured by water flowrate and temperature difference. The average measurement error of server workload is±10%. Rack inlet/exhaust air temperature is measured by thermocouples, with the average measurement error of±0.5 °C. Water mass flowrate is measured by flowmeter, with the average measurement error of±15%.

A certain deviation (8%–10%) is observed between the predicted *EER* and the measured value. It is mainly caused by the measurement error of water flowrate (±15%), which affects the measurement of cooling load.

For each testing condition, the inlet and exhaust air temperature of all 60 racks are measured. The measured temperature of inlet/exhaust air is 22.7 °C–26.6°Cin summer and 22.8 °C–26.8°Cin winter, with the maximum deviation within 4 °C, which is in line with design goals.

For each rack workload, Fig. 8 shows the measurement deviation of water temperature, water flowrate and energy efficiency EER.

The measurement deviation of inlet water temperature is illustrated by Fig. 8(a), with the maximum deviation of 0.7°Cin summer and 1.1 °C in winter. Considering the average temperature measurement error as±0.5 °C, such deviation can be accepted.

The normalized flowrate measurement deviation is illustrated by Fig. 8(b). The maximum deviation in summer is 12.2%, and 9.5% in winter. Considering the average flowrate measurement error as±15%, such deviation can be accepted.

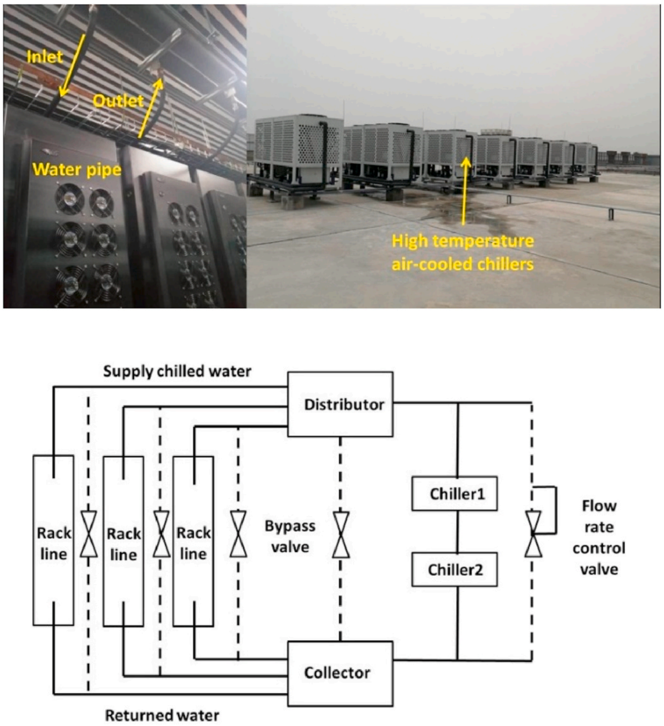

Fig. 7. Photo and schematic diagram of the testing water loop.

Table 2
Exergy optimal performance in summer (typical outdoor air dry/wet bulb temperature of 31 °C/26 °C).

Percentage of rack workload	Optimal inlet water temperature	Optimal water flow rate	Cooling load undertaken by chiller 1	Cooling load undertaken by chiller 2	Bypass cooling load	Optimal *EER*
30%	22.3 °C	921 kg/h	0	79%	21%	9.6
60%	20.9 °C	1752 kg/h	27%	59%	14%	8.5
80%	19.6 °C	2239 kg/h	35%	55%	10%	7.8
100%	18.2 °C	2871 kg/h	41%	53%	6%	7.2

Table 3
Exergy optimal performance in winter (typical outdoor air dry/wet bulb temperature of -12 °C/-14.5 °C).

Percentage of rack workload	Optimal inlet water temperature	Optimal water flow rate	Cooling load undertaken by chiller 1	Cooling load undertaken by chiller 2	Bypass cooling load	Optimal *EER*
30%	22.3 °C	921 kg/h	0	52%	48%	11.9
60%	20.9 °C	1752 kg/h	16%	47%	37%	11.2
80%	19.6 °C	2239 kg/h	28%	41%	31%	10.5
100%	18.2 °C	2871 kg/h	35%	38%	27%	9.7

Fig. 8(c) shows the measurement deviation of *EER* for the double-chiller unit. Compared with the optimal values, the maximum deviation percentage is 13.5% in July 2018, and 10.3% in January 2019. This is mainly caused by the measurement deviation of chiller cooling load and the bypass cooling load. As for energy saving potential assessment, *EER* measurement deviation less than 15% is also acceptable.

6. Conclusion

The main conclusions are summarized as follows :

(1) Given the zero-exergy state and heat exchanger area, the exergy destruction of rack-level water-cooling infrastructure mainly depends on fluid flowrate, number of heat exchangers and *NTU* allocations.

Table 4
Measured performance from July 20th to 28th, 2018(measured outdoor air dry bulb temperature of 23.7–31.5 °C).

Percentage of rack workload	Tested inlet water temperature	Tested water flow rate	Mean inlet/exhausted air temperature of rack line 1/line 2/line 3	Cooling load percentage of chiller 1/2	Bypass cooling load percentage	Tested *EER*
31.6%	22.8 °C	1035 kg/h	Mean inlet air temp: 23.9 °C/24.5 °C/24.8 °C Mean exhaust air temp: 24.6 °C/25.1 °C/23.8 °C	0/81.4%	18.6%	8.3
62.1%	21.2 °C	1869 kg/h	Mean inlet air temp: 24.1 °C/24.8 °C/25.3 °C Mean exhaust air temp: 23.7 °C/25.4 °C/24.5 °C	32.1%/55.2%	12.7%	7.6
78.3%	19.0 °C	2106 kg/h	Mean inlet air temp: 25.0 °C/24.2 °C/23.7 °C Mean exhaust air temp: 23.9 °C/23.6 °C/25.8 °C	36.2%/51.3%	12.5%	7.2
98.2%	17.5 °C	3077 kg/h	Mean inlet air temp: 24.6 °C/25.0 °C/25.9 °C Mean exhaust air temp: 24.1 °C/23.6 °C/23.8 °C	45.4%/49.0%	5.6%	6.5

Table 5
Measured performance from January 15th to 23rd, 2019(measured outdoor air dry bulb temp of -16.5 °C ~ -9.8 °C).

Percentage of rack workload	Tested inlet water temperature	Tested water flow rate	Mean inlet/exhausted air temp of rack line 1/line 2/line 3	Cooling load percentage of chiller 1/2	Bypass cooling load percentage	Tested *EER*
33.2%	21.4 °C	873 kg/h	Mean inlet air temp: 24.3 °C/24.9 °C/23.8 °C Mean exhaust air temp: 24.8 °C/25.3 °C/24.7 °C	0/49.6%	50.4%	11.0
58.8%	19.8 °C	1586 kg/h	Mean inlet air temp: 24.4 °C/23.9 °C/25.1 °C Mean exhaust air temp: 25.1 °C/24.6 °C/24.8 °C	14.5%/48.2%	37.3%	10.4
78.9%	20.7 °C	2107 kg/h	Mean inlet air temp: 25.3 °C/23.8 °C/23.6 °C Mean exhaust air temp: 23.9 °C/24.3 °C/24.2 °C	27.3%/43.5%	29.2%	10.6
97.1%	18.9 °C	2981 kg/h	Mean inlet air temp: 23.8 °C/24.6 °C/25.2 °C Mean exhaust air temp: 24.2 °C/23.7 °C/24.5 °C	39.0%/35.6%	25.4%	8.7

(2) The double-heat-exchanger configuration shows smaller exergy destruction than single-heat-exchanger configuration. The best exergy performance occurs with the front door and rear door fan-coil area of 0.2/0.8.
(3) For a10kW loaded rack, the optimal double-heat-exchanger cooling infrastructure provides 152W extra cooling capacity at most, which helps to reduce the *PUE* value by about 3.5% for the data center.
(4) Measured *EER* of the double-chiller configuration is 7%–18% higher than that of single-chiller.
(5) Measured best performance of the combined water loop and the rack-level water-cooling infrastructure shows a good agreement with the optimal performance predicted by the exergy model, which validates both the exergy analysis method and the minimum exergy destruction law on rack-level cooling design and optimization.

7. Outlook and perspectives

The exergy-based analysis has been proved feasible on the optimal design of rack-level effective cooling infrastructures. Recent research shows the minimum exergy destruction law also works on data center combined power management, which can guide the optimization from chip-level power usage to room-level power allocation and find more energy saving potentials. The scalable exergy model can cover all the heat transfer paths, thermal behavior and operating parameters in data centers. The exergy model plays an increasingly important role in improving the comprehensive performance of data center, creating more suitable thermal environment, saving more energy, finding more effective operation strategy and decreasing the *PUE*. Exergy analysis and optimization method provides a useful and powerful tool for future green data center operation and management.

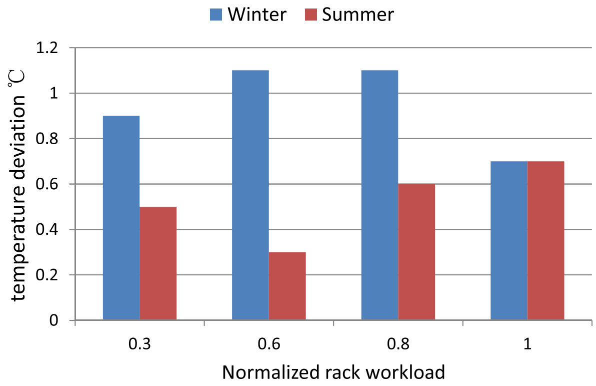

(a) inlet water temperature

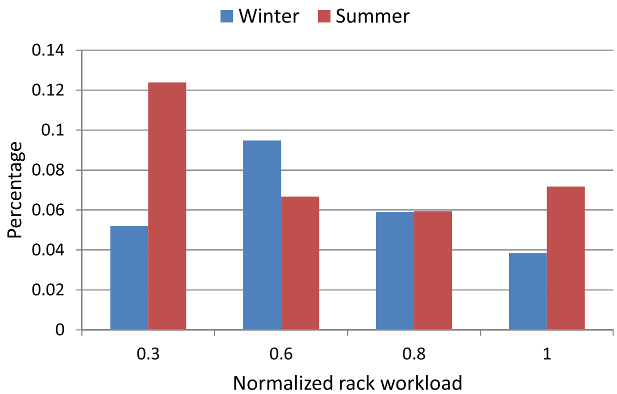

(b) **normalized water flowrate**

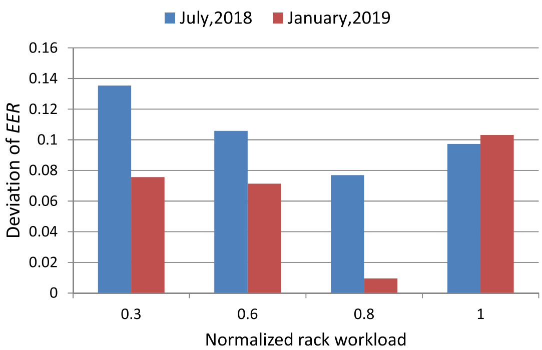

(c) *EER* deviation for the double-chiller unit during the testing

Fig.8 Measurement deviations

Fig. 8. Measurement deviations.

Author statement

I have made substantial contributions to the conception or design of the work; or the acquisition, analysis, or interpretation of data for the work; AND I have drafted the work or revised it critically for important intellectual content; AND I have approved the final version to be published; AND I agree to be accountable for all aspects of the work in ensuring that questions related to the accuracy or integrity of any part of the work are appropriately investigated and resolved.

Declaration of competing interest

The authors declare that they have no known competing financial interests or personal relationships that could have appeared to influence the work reported in this paper.

Acknowledgments

This work was supported by the Strategic Priority Research Program of Chinese Academy of Sciences (Grant No. XDA17010205).

References

[1] M. Dayarathna, Y. Wen, R. Fan, Data center energy consumption modeling: a survey, IEEE Commun. Surv. Tutorials 18 (1) (2016) 732–794.
[2] S. Patankar, Air flow and cooling in a data center, J. Heat Tran. 132 (7) (2010) 1–17.
[3] R.R. Sharma, C.E. Bash, C.D. Patel, Dimensionless parameters for evaluation of thermal design and performance of large-scale data centers, in: Proceeding of the Eighth ASME/AIAA Joint Thermophysics and Heat Transfer Conference, 2002. St Louis Missouri.
[4] M.K. Herrlin, Rack cooling effectiveness in data center and telcom central offices: the rack cooling index (RCI), Build. Eng. 111 (2) (2005) 1–11.
[5] M.K. Herrlin, Improved Data Center Energy Efficiency and Thermal Performance by Advanced Air Flow Analysis, Digital Power Forum, San Francisco, California, 2007.
[6] A.J. Shah, V.P. Carey, C.E. Bash, et al., An open-system, exergy-based analysis of major data center thermal management components, in: Advanced Technology Workshop on Thermal Management Hosted by the International Microelectronics and Packaging Society, IMAPS), Palo Alto, California, 2004.
[7] A.J. Shah, V.P. Carey, C.E. Bash, et al., An exergy-based control strategy for computer room air-conditioning units in data centers, in: Proceeding of 2004 ASME International Mechanical Engineering Congress and Exposition (IMECE2004-61384), Anaheim, California, 2004.
[8] A.J. Shah, V.P. Carey, C.E. Bash, et al., Exergy-based optimization strategies for multi-component data center thermal management: part I, analysis, in: Proceedings of International Electronic Packaging Technical Conference and Exhibition (IPACK2005-73137), 2005. San Francisco, California.
[9] A.J. Shah, V.P. Carey, C.E. Bash, et al., Exergy-based optimization strategies for multi-component data center thermal management: part II, Application and validation, in: Proceeding of International Electronic Packaging Technical Conference and Exhibition (IPACK2005-73138), 2005. San Francisco, California.
[10] A.J. Shah, V.P. Carey, C.E. Bash, et al., An open-system, exergy-based analysis of major data center thermal management components, in: Advanced Technology Workshop on Thermal Management Hosted by the International Microelectronics and Packaging Society, IMAPS), Palo Alto, California, 2004.
[11] A.J. Shah, V.P. Carey, C.E. Bash, et al., An exergy-based control strategy for computer room air-conditioning units in data centers, in: Proceeding of 2004 ASME International Mechanical Engineering Congress and Exposition (IMECE2004-61384), Anaheim, California, 2004.
[12] A.J. Shah, V.P. Carey, C.E. Bash, et al., Exergy-based optimization strategies for multi-component data center thermal management: part I, analysis, in: Proceedings of International Electronic Packaging Technical Conference and Exhibition (IPACK2005-73137), 2005. San Francisco, California.
[13] A.J. Shah, V.P. Carey, C.E. Bash, et al., Exergy-based optimization strategies for multi-component data center thermal management: part II, Application and validation, in: Proceeding of International Electronic Packaging Technical Conference and Exhibition (IPACK2005-73138), 2005. San Francisco, California.
[14] A.J. Shah, V.P. Carey, C.E. Bash, et al., Exergy analysis of data center thermal management systems, J. Heat Tran. 130 (2) (2008), 021401–021410.
[15] A.J. Díaz, R. Caceres, J.M. Cardemil, L. Silva-Llanca, Energy and exergy assessment in a perimeter cooled data center: the value of second law efficiency, Appl. Therm. Eng. 124 (2017) 820–830.
[16] R. Khalid, A.P. Wemhoff, Y. Joshi, Energy and exergy analysis of modular data centers, IEEE Trans. Compon. Packag. Manuf. Technol. 7 (2017) 1440–1452.
[17] X. Qian, Z. Li, Z. Li, Entransy and exergy analyses of air flow organization in data centers, Int. J. Heat Mass Tran. 81 (2015) 252–259.
[18] A.J. Shah, V.P. Carey, C.E. Bash, C.D. Patel, Exergy analysis of data center thermal management systems, J. Heat Tran. (2008) 130.
[19] A. Bhalerao, K. Fouladi, L. Silva-Llanca, A.P. Wemhoff, Rapid prediction of exergy destruction in data centers due to air flow mixing, Numer. Heat Tran., Part A: Applications 70 (2016) 48–63.
[20] K. Fouladi, A.P. Wemhoff, L. Silva-Llanca, K. Abbasi, A. Ortega, Optimization of data center cooling efficiency using reduced order flow modeling within a flow network modeling approach, Appl. Therm. Eng. 124 (2017) 929–939.
[21] L. Silva-Llanca, A. Ortega, K. Fouladi, M. del Valle, V. Sundaralingam, Determining wasted energy in the airside of a perimeter-cooled data center via direct computation of the Exergy Destruction, Appl. Energy 213 (2018) 235–246.
[22] L. Silva-Llanca, M. del Valle, A. Ortega, A.J. Díaz, Cooling effectiveness of a data center room under overhead air flow via entropy generation assessment in transient scenarios, Entropy 21 (2019) 98.
[23] L. Silva-Llanca, M. del Valle, A. Ortega, The effectiveness of data center overhead cooling in steady and transient scenarios: comparison of downward flow to a cold aisle versus upward flow from a hot aisle, in: ASME 2015 International Technical Conference and Exhibition on Packaging and Integration of Electronic and Photonic Microsystems Collocated with the ASME 2015 13th International Conference on Nanochannels, Microchannels, and Mini channels, 2015.
[24] H. Moazamigoodarzi, S. Pal, S. Ghosh, I.K. Puri, Real-time temperature predictions in IT server enclosures, Int. J. Heat Mass Tran. 127 (2018) 890–900.
[25] S. Pal, H. Moazami-goodarzi, S. Ghosh, K. Thorn, I.K. Puri, in: Plate-fin Heat Exchanger Suitable for Rack-Mountable Cooling Unit, Google Patents, 2019.
[26] H. Moazamigoodarzi, S. Pal, D. Down, M. Esmalifalak, I.K. Puri, Performance of A Rack mountable cooling unit in an IT server enclosure, Ther. Sci. Eng. Progress (2019) 100–395.
[27] J. Priyadumkol, C. Kittichaikarn, Application of the combined air-conditioning systems for energy conservation in data center, Energy Build. 68 (2014) 580–586.
[28] H. Moazamigoodarzi, R. Gupta, S. Pal, P.J. Tsai, S. Ghosh, I.K. Puri, Modeling temperature distribution and power consumption in IT server enclosures with row-based cooling architectures, Appl. Energy 261 (2020) 114–355.
[29] A.J. Shah, Exergy-based Analysis and Optimization of Computer Thermal Management Systems, Ph.D Thesis, University of California, Berkeley, Fall, 2005.